Results in Engineering 24 (2024) 102920

Contents lists available at ScienceDirect

Results in Engineering

journal homepage: www.sciencedirect.com/journal/results-in-engineering

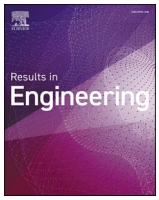

Evaluation of the hydrogen/oxygen and thermoelectric production of a hybrid solar PV/T-electrolyzer system

Armel Zambou Kenfack [a], Modeste Kameni Nematchoua [a], Venant Sorel Chara-Dackou [a,b,*], Elie Simo [a]

[a] Energy and Environment Laboratory, Department of Physics, Faculty of Science, University of Yaoundé I, PO Box 812, Cameroon
[b] Carnot Energy Laboratory (CEL), Department of Physics, Faculty of Science, University of Bangui, PO Box 1450, Bangui, Central African Republic

ARTICLE INFO

Keywords:
Solar PV/T system
Electrolyzer
Hydrogen production
Thermoelectric production
Exergy optimization

ABSTRACT

In order to achieve a sustainable, low-carbon energy future, it is necessary to develop innovative and integrated solutions. However, one of the main obstacles to the advancement of renewable energy is storage. With this in mind, hybrid systems combining solar energy and hydrogen production have great potential. This article focuses on the evaluation of a solar PV/T (photovoltaic-thermal) system coupled with an electrolyser for the joint production of hydrogen and heat. Simulations are performed in MATLAB. The analysis reveals that with PV/T power supply, the production potential is estimated at 179.6 W and 551.9 W respectively for electrical and thermal power. An in-depth study aimed at optimizing the system by evaluating the quality of the energy used in the water electrolysis process makes it possible to analyze the effect of certain operating parameters. With a water flow of 5.7 $\times 10^{-3}$ m^3/h, a current density of 200 mA/ cm^2 and an electrolyzer temperature of 60 °C, the monthly production of hydrogen and oxygen reaches the maximum values of 4.85 m^3 and 2.42 m^3 respectively. This led to a maximum exergy efficiency of 57.8 %. This study demonstrates the linearity between hydrogen production and current density which at high density reduces exergy performance.

1. Introduction

The transition to renewable and sustainable energy sources has become a global priority to address the environmental and energy challenges we face [1,2]. Moreover, gathered at the Conference of the Parties (COP), several countries have set themselves the objective of reducing their greenhouse gas (GHG) emissions by 2100 to keep global warming below 2 °C. Faced with energy storage problems, hydrogen has emerged as a promising energy vector, capable of storing and transporting energy efficiently and cleanly [3]. According to several studies [4,5], it is predicted that electricity, synthetic fuels and hydrogen will represent 32 % of the global energy composition. This share should then increase by 50 % by 2050. Hydrogen has many applications for example hydrogen fuel cell vehicles, hydrogen powered phones and many others [6]. In fact, a PEM electrolyzer (Polymer electrolyser membrane) can achieve an efficiency of 95.1 % at 300 bar pressure and high temperature [7]. Hospitals and several sectors of activity today encounter a real problem with oxygen and heating. And hydrogen is considered in its current state as the energy potential of the future [8]. It is an energy that is abundant in the universe, but is not available in pure form on earth [9]. Especially since the PV system generates direct current which is directly used by the electrolyser. At the same time, heat production represents a significant share of global energy consumption, particularly in the residential and industrial sectors [10]. The coupling of hydrogen and heat production from renewable sources such as photovoltaic-thermal solar (PVT) offers interesting prospects for responding to these challenges [11,12]. PVT systems combine the production of electricity through photovoltaic cells and the production of heat by recovery of waste heat from the PV panel. This helps improve the overall system efficiency and generate both electricity and heat from a single installation [13]. When these PV/T systems are coupled to an electrolyzer, it becomes possible to produce renewable hydrogen while benefiting from the synergies between the heat and electricity generated [14,15].

Much research has been carried out on the production of electricity, hydrogen and heat in solar systems. Mokhtara et al. [16] proposed a multi-criteria optimization method to find the optimal sizing of a PV-electrolyzer system according to technical and financial constraints.

* Corresponding author. Energy and Environment Laboratory, Department of Physics, Faculty of Science, University of Yaoundé I, PO Box 812, Cameroon.
E-mail address: chav7@yahoo.com (V.S. Chara-Dackou).

https://doi.org/10.1016/j.rineng.2024.102920
Received 23 July 2024; Received in revised form 5 September 2024; Accepted 16 September 2024
Available online 20 September 2024

The demand effect H_2 evaluated revealed that the Grid/-PV/Electrolyser/fuel cell and storage tank combination is better with a COE (cost of energy) of $0.1 per kWh. The authors [17] carried out a modeling of the PV-electrolyzer and Wind turbine-electrolyzer system. Using Matlab software, their study demonstrated that it is possible to achieve a hydrogen production of 0.55 Nm^3/h with PV and 0.675 Nm^3/h with wind turbines in a coastal region of Cameroon. In the same vein, the authors of ref [18]. reveal in their study that with a PV area of 160 m^2 coupled to hydrogen is the best configuration compared to the PV/battery system to satisfy a load of 19,745 kWh/year leading to a COE of 1.06 $/kWh for a payback period of 6.44 years. The authors of ref [19]. carried out a study aimed at solving the problem of maximum voltage-power matching of PV to the operating voltage of the electrolyzer. Several studies have also shown that the water temperature and the number of cells in the electrolyzer considerably affect the output voltage of PEM electrolysis [20,21]. This voltage is also considerably affected by the operating temperature of the electrolyzer. This requires optimization of system parameters. The authors [22] were able, thanks to an exergy analysis and a multi-objective optimization algorithm, that the power of the solid oxide fuel cell and gas turbine and electrolyzer loses approximately 61 % of the exergy which enters the electrolyzer of the Panels PV. A similar study [23] carried out rather with the PV/T source showed that the PV/T system reached an exergy efficiency of 15.8 % while that of the electrolyzer reached 60.7 % at a current density of 400 mA/cm^2 and at a water temperature of 45.8 °C. Thus establishing that the exergy efficiency increases with the water temperature but on the other hand decreases with the current density. The authors of ref [24]. followed suit by searching for optimal parameters such as the tilt angle of the PV panel. The authors of ref [25]. carried out a more in-depth study on the suitable type of PV cells for hydrogen production. Their study reveals that polycrystalline cells are cost-effective than monocrystalline and amorphous silicon cells for hydrogen production. A solar-electrolyzer system for the production of electricity thanks to the rankine cycle and cold by a refrigeration system is presented in ref [26].. An overall exergy efficiency of 2082 % was obtained. At the same time, the authors [27–29] demonstrated the need to perform exergy optimization of solar-electrolyzer technologies. An exergy analysis of the photovoltaic concentrator (CPV) system reveals that there is more loss in the CPV than in the electrolyzer [30].

Although previous work has brought significant advances in the study of hybrid PV/T systems coupled with hydrogen production, several gaps remain in the literature. First of all, the majority of studies do not take advantage of the thermal energy recovered by the PV/T panel to power the electrolysis process, thus limiting the overall efficiency of the system. Furthermore, no PV/T system model integrated into the HOMER Pro simulation tool has been developed so far, preventing an in-depth techno-economic evaluation of these solutions. Finally, there are few works that analyze in detail the influence of essential design parameters such as energy storage capacity or electrical losses in the electrolytic system, although they are crucial for system optimization. It is in this context that this study takes place, aiming to fill these gaps and contribute to a better understanding and optimization of solar PV/T systems coupled with the production of hydrogen and heat. Table 1 gives the precise limits between the work from the literature and the contribution of the present study. The main contributions of this study are as follows:

- Modeling and simulation of a hybrid PV/T-electrolyzer solar system;
- The influence of solar irradiation and ambient temperature on the IV characteristics of the PV/T hybrid system is presented;
- The electrical and thermal productivity of the PV/T system is analyzed;
- Integration of the PV/T system in the production of clean hydrogen;
- Evaluation of hydrogen and oxygen production;
- Exergy optimization of the hybrid PV/T-electrolyzer system.

This article is organized as a continuation after this introductory section, section 1, will follow section 2 entitled methodology, then section 3 entitled results and discussion and then section 4 to conclude.

2. Methodology

2.1. Physical model

The PV/T -Electrolyzer device is presented in Fig. 1. It is made up of a water pump which supplies the PV/T and the electrolyser. A commercial PEM type electrolyzer was used to generate hydrogen and oxygen. A DC/DC step-down converter was used to adjust the voltage of the PV/T to provide the power required by the PEM electrolyzer. The PV/T system captures solar energy and converts it into electricity and heat. This will involve circulating a fluid (water) below the PV to recover the heat from this fluid and use it in the electrolyzer for the production of hydrogen and oxygen. The inclusion of a heat exchanger in the system serves to recover the heat produced by the photovoltaic panels. When PV cells operate, part of the solar energy is converted into heat rather than electricity. The heat exchanger makes it possible to recover this residual heat to use it, for example for heating domestic water. This improves the overall efficiency of the system by making best use of the captured solar energy. The reinjection of the heat produced by the electrolysis reactions itself makes it possible to maintain an inlet temperature range between 60 °C and 80 °C. A compressor is used to store products in storage tanks. Thermal production from the PV/T system is also stored in storage tanks. The characteristics of each system are presented in Tables 2 and 3.

2.2. Mathematical model

2.2.1. Hybrid PV/T solar system

Much research has focused on creating mathematical models to simulate the electrical behavior (the relationship between current and

Table 1
Limit of existing work in the literature.

Study	Solar hydrogen production	Software	Energy source	Electricity production	Heat production	Evaluation of monthly oxygen production	Evaluation of monthly hydrogen production	Exergy Optimization
Present study	✓	**MATLAB**	**PV/T**	✓	✓	✓	✓	**3 parameters**
[7]	✓	MATLAB	PV	✓	×	×	✓	×
[17]	✓	MATLAB	PV	✓	×	×	✓	×
[23]	✓	MATLAB	PV/T	✓	✓	×	✓	**2 parameters**
[24]	✓	MATLAB	PV	✓	×	×	×	×
[25]	✓	MATLAB	PV	✓	×	×	×	×
[31]	✓	//	PV/FC	✓	✓	✓	✓	×
[32]	✓	MATLAB	PV/T	✓	✓	×	✓	×
[33]	✓	MATLAB	PV	✓	×	×	✓	×
[40]	✓	MATLAB	PV	✓	×	×	✓	×
[41]	✓	TRNSYS	PV	✓	×	×	✓	×

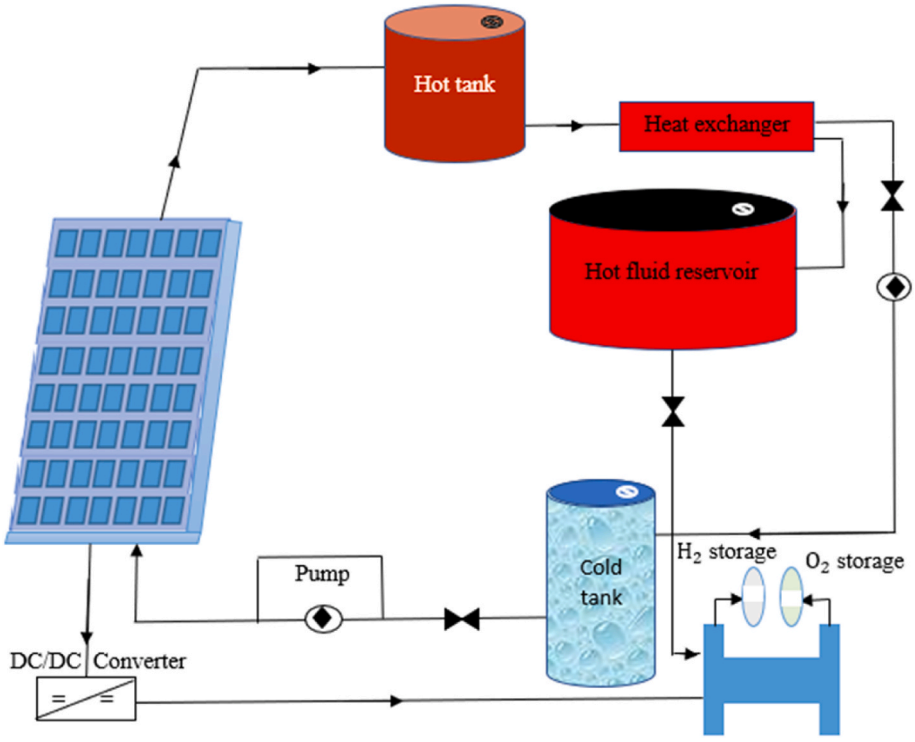

Fig. 1. Presentation of the PV/T-Electrolyzer system.

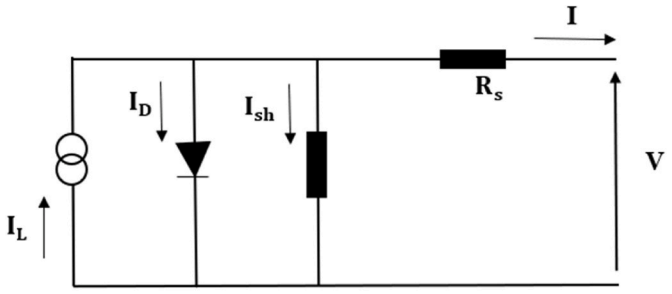

Fig. 2. Electrical diagram of a PV cell.

Table 2
Electrolyzer input data [24].

Settings	Symbols	Values
Reversible voltage	V_{rev} (V)	1229
Chemical Exergy of hydrogen	$ex_{ch_{H2}}$ (KJ/kg)	159.13
Chemical Exergy of oxygen	$ex_{ch_{O2}}$ (KJ/kg)	0
Chemical Exergy of water	$ex_{ch_{H2O}}$ (KJ/kg)	2.5
The area of the electrode	A_e (m^2)	0.25
Faraday's constant	F(C/mol)	96485
number of electrons	Z	2
Coefficient of overvoltage of the electrode	s (V)	0.185
	t_1 ($A^{-1}m^2$)	1.002
	t_2 ($A^{-1}m^2$C)	8424
	t_3 ($A^{-1}m^2$ C)	247.3
ohmic resistance of the electrolyzer	r_1 (Ωm^2)	$8.05e^{-5}$
	r2) (Ωm^2C^{-1})	$-2.5e^{-7}$
f_1 (mA^2cm^{-4})		200
f_2 (mA^2cm^{-4})		0.985

voltage) of solar cells, photovoltaic modules or photovoltaic generators. In other words, on the one hand there have been efforts to model the fundamental characteristics of photovoltaic components at the electrical level, and on the other hand work aimed at modeling their overall energy production. The following paragraph will consist of modeling the current-voltage characteristic of solar cells.

Table 3
PV/T hybrid solar system data [17].

PW-180	12 V configuration
Typical power (W) (1000 W/m^2, 25 °C)	180
Vmax (V)	35
Imax (A)	3.55
Short circuit current (A) Isc	4.45
Open circuit voltage(V) Voc	43.5
The area of the PV/T (m^2)	0.8

- Current-voltage characteristic of the PV/T system

Fig. 2 presents the photovoltaic cell model used in this study. It is a single diode model. Based on this equivalent electrical diagram of the PV cell, we can apply the laws of currents to the nodes of the circuit to establish the equation linking the current and the voltage of the cell [28]. The PV output current I can be given by **equation (1)**.

$$\mathbf{I} = I_L - I_D - I_{sh} \quad (1)$$

Or I_L is the photocurrent and **I_D** the diode current given by **equation (2)**. **I_{sh}** is the shunt leakage current given in **Equation (3)** . In the expression for the diode current, **I_O** is the saturation current and V is the terminal voltage of the solar cell, A is the ideality factor and **R_s** is the series resistance, k is the Boltzmann constant, q is the elementary charge of the electron and Tc is the absolute temperature of the solar cell [32, 33].

$$I_D = I_O\left(e^{\left(\frac{(V+I.R_s)q}{A.K.T_c}\right)} - 1\right) \quad (2)$$

$$I_{sh} = \frac{V + I.R_s}{R_{sh}} \tag{3}$$

Substituting equation (2) and **equation (3)** into **Equation (1)** we obtain **Equation (4)** [2].

$$I = I_L - I_O\left(e^{\left(\frac{(V+I.R_s)q}{A.K.T_c}\right)} - 1\right) - \frac{V + I.R_s}{R_{sh}} \tag{4}$$

Neglecting the leakages in the PV module, the resistance and the shunt current tend to infinity and zero respectively and equation (5) [21] is obtained.

$$I = I_L - I_O\left(e^{\left(\frac{(V+I.R_s)q}{A.K.T_c}\right)} - 1\right) \tag{5}$$

In the case of the short circuit, the output voltage is zero (V = 0) and the resulting expression is given in **equation (6)** [8]:

$$I_{cc} = I_L - I_O\left(e^{\left(q\frac{I_{cc}.R_s}{A.K.T_c}\right)} - 1\right) \tag{6}$$

In the case of an open circuit, no current flows (I = 0) and the photoelectric current is expressed in **equation (7)** [31][35].

$$I_L = I_O\left(e^{\left(q\frac{V_{oc}}{A.K.T_c}\right)} - 1\right) \tag{7}$$

The maximum current is obtained at the maximum power point given in **equation (8)** [17].

$$I_m = I_L - I_O\left(e^{\left(\frac{(V_m+I_m.R_s)q}{A.K.T_c}\right)} - 1\right) \tag{8}$$

By inserting the logarithm function into **equation (8)**, we obtain equation **(9)**:

$$\ln\left(\frac{I_L - I_m}{I_0}\right) = q\frac{V_m + I_m.R_s}{A.K.T_c} \tag{9}$$

By applying the same function to equation (7) and subtracting with equation **(9)**, the new expression is given in **equation (10)**. Then a rearrangement allows us to have equation **(11)**.

$$\ln\left(\frac{I_L - I_m}{I_0}\right) - \ln\left(\frac{I_L}{I_0}\right) = q\frac{V_m + I_m.R_s}{A.K.T_c} - q\frac{V_{oc}}{A.K.T_c} \tag{10}$$

$$\ln\left(\frac{I_L - I_m}{I_L}\right) = \frac{q}{A.K.T_c}(V_m + I_m.R_s - V_{oc}) \tag{11}$$

This results in the expression for the series resistance $\mathbf{R_s}$ given in **equation (12)** [19]. The output power is expressed in **equation (13)** [32].

$$R_s = \frac{\frac{A.K.T_c}{q}\ln\left(1 - \frac{I_m}{I_L}\right) + V_{oc} - V_m}{I_m} \tag{12}$$

$$P_{elect} = I.V \tag{13}$$

At the maximum power point, the power is at its maximum, so its derivative with respect to the voltage is zero $dP_{elct}/dV = 0$. In this case, the expression for the ideality factor A takes the form of **equation (14)** **[33]**.

$$A = \frac{q(2V_m - V_{oc})}{n_s KT\left(\frac{I_{sc}}{I_{cc} - I_m} + \ln\left(1 - \frac{I_m}{I_{cc}}\right)\right)} \tag{14}$$

The system voltage can therefore be expressed by **equation (15)** [21].

$$V = -I.R_s + \frac{q}{AKT}\ln\left(\frac{-I + I_{cc} + I_0}{I_0}\right) \tag{15}$$

Likewise, the thermal power P_{th} of the system is expressed by **equation (16)**. With m_f, C_f, T_{fo} and T_{fs} represent the flow rate of the fluid, its specific capacity, the inlet and outlet temperature respectively [13]. More details are given in Refs. [13,34].

$$P_{th} = m_f.C_f.(T_{fo} - T_{fi}) \tag{16}$$

2.2.2. PV/T-electrolyzer coupled system

Polymer membrane electrolyzers are manufactured from pure polymer membranes or composite membranes. In the latter, the different materials are assembled to form a polymer matrix. The most commonly used material for these membranes is Nafion (very effective in energy storage due to its high efficiency) [9]. Its principle results from the electrolysis of water which is the process used to produce hydrogen and oxygen from an electrolyzer [4,38,43].

The electrolyzer is made up of two electrodes (cathode (−) and anode (+)) immersed in water. When an electric current is applied between the two electrodes, a redox phenomenon occurs: hydrogen gas is released at the cathode when the water is reduced while at the anode gaseous oxygen is released during the oxidation of hydroxide ions. This is described by equation **(17)** and **equation (18)** representing the half-reactions [5,6].

- At the cathode, water is reduced, releasing hydrogen gas:

$$2H_2O + 2\,e^- \rightarrow H_2 + 2\,OH^- \tag{17}$$

- At the anode, hydroxide ions are oxidized, releasing oxygen gas:

$$4\,OH^- \rightarrow O_2 + 2H_2O + 4\,e^- \tag{18}$$

The PEM model considered in this study is based on single-cell characteristics. Using the Ulleberg model. Its voltage depends on three parameters as defined in **equation (19)** [22].

$$V_{cell} = V_{rev} + V_{act} + V_{ohm} \tag{19}$$

Where V_{rev} is the reversible overvoltage necessary to overcome the thermodynamic limitations of the electrolysis process and allow the production of gases (hydrogen and oxygen). Its value is available in Table 2. The term V_{act} is the activation overvoltage (**equation (20)**) making it possible to activate the electrochemical reactions at the electrodes. Next, V_{ohm} is the ohmic overvoltage (**equation (21)**) which in fact represents the voltage lost due to the electrical resistance of the different components of the electrolyzer cell [17,40].

$$V_{act} = \text{slog}\left(\frac{t_1 + \frac{t_2}{T} + \frac{t_3}{T^2}}{A_e}I + 1\right) \tag{20}$$

$$V_{ohm} = \frac{r_1 + r_2 T}{A_e}I \tag{21}$$

The terms t and r represent the overvoltage coefficients and the ohmic resistances, respectively. The hydrogen production rate can be evaluated as follows by **equation (22)** [41].

$$\dot{m}_{H_2} = \eta_F\frac{I}{zF} \tag{22}$$

With η_F representing the Faraday efficiency which is deduced from an empirical development expressed in **equation (23)** [39].

$$\eta_F = \frac{\left(\frac{I}{A_e}\right)^2}{f_1 + \left(\frac{I}{A_e}\right)^2} f_2 \tag{23}$$

- Expression of the exergy of the system

Exergy is an important concept in thermodynamics that helps evaluate the quality and utility of a form of energy. It represents the maximum amount of useful work that can be obtained from a system or flow of energy when it is brought from its initial state to the state of thermodynamic equilibrium with the environment. Unlike energy, which is always conserved, exergy can be destroyed during irreversible transformations. Exergy takes into account both the energy and the entropy of the system, and therefore makes it possible to evaluate its quality and its potential for conversion into useful work [34–36], [42]. The importance of an exergy efficiency assessment for this system can be listed as follows:

- In an electrolysis system, the electricity supplied is a high quality form of energy (high exergy) that is used to break down water into hydrogen and oxygen;
- However, the electrolysis process involves irreversibilities (heat losses, resistance, etc.) which reduce the exergy of the system.
- Evaluating the exergy efficiency of an electrolyzer makes it possible to quantify the fraction of the exergy supplied which is actually converted into exergy of the products (hydrogen and oxygen).
- This gives a better indication of the actual performance of the system than traditional energy efficiency, which does not take into account exergy losses.

exergy efficiency of a PEM electrolyzer is defined as the ratio between the exergy gained by the reaction products (difference in exergy of the reactants reacting with the exergy of the products) and the exergy supplied in the form of electricity at the entrance to the system. Expressed in **equation (24)** [36,37].

$$\eta_{ex} = \frac{(\dot{E}_{H_2} + \dot{E}_{O_2}) - (\dot{E}_{H_2O})}{P_{elect}} \tag{24}$$

With the exergy of the reactant and products given respectively by **equations (25)–(27)** [21–23].

$$\dot{E}_{H_2O} = \dot{m}_{H_2O}\left(ex_{ch} + ex_{ph}\right)_{H_2O} \tag{25}$$

$$\dot{E}_{H_2} = \dot{m}_{H_2O}\left(ex_{ch} + ex_{ph}\right)_{H_2} \tag{26}$$

$$\dot{E}_{O_2} = \dot{m}_{O_2}\left(ex_{ch} + ex_{ph}\right)_{O_2} \tag{27}$$

The chemical exergy of the different constituents is given in Table 2. And their physical exergy is expressed by **equation (28)** [23].

$$ex_{ph} = C_P.T_a\left(\frac{T}{T_a} - 1 - \ln\left(\frac{T}{T_a}\right) + \ln\left(\frac{P}{P_0}\right)^{(k-1)/k}\right) \tag{28}$$

2.3. Digital model

The meteorological data used in this study are those of an equatorial climate in Cameroon, more precisely from the town of Bafoussam available in ref [13].. The numerical method is based on an explicit scheme for temporal discretization, which allows a simple and efficient implementation in MATLAB. Table 3 shows the input data of the solar PV/T system. The parameters of the heat transfer fluid which is water in this case are available in ref [13]..

3. Results and discussion

This section focuses on the presentation of the results obtained. The influence of cell temperature and solar irradiation on the current-voltage characteristics of the hybrid solar system is evaluated. In addition, the thermal and electrical performances are analyzed and the productivities of the hybrid solar PV/T-electrolyzer system as well as an exergy optimization are carried out.

- ***Validation***

To validate the numerical model of the electrolyzer powered by the PV/T hybrid solar system, the current-voltage characteristics of the electrolyzer are compared with the experimental results. This to guarantee the reliability of the model presented here, the current is taken as a fixed reference and the errors between the experimental and numerical voltages are evaluated. In Table 4 we can observe that the root mean square error (RMSE) is 0.54 % and the relative error (RE) is 1.28 %. These values are very low, indicating that the numerical model very accurately represents the experimental behavior of the electrolyzer. Showing that the model captures the main physical and electrochemical phenomena that govern the operation of the system.

- Influence of temperature on current-voltage and power characteristics of the PV/T system

Fig. 3 allows you to visualize how cell temperature affects the current-voltage characteristics of the PV/T system. It should be observed that as the cell temperature increases, the output voltage decreases. With a maximum cell temperature at 60 °C, the voltage is 44.32 V and the maximum current intensity is 4.39 A. On the other hand, with a minimum cell temperature at 15 °C, the maximum voltage is 57.56 V and the current maximum is 0.07 A. This is explained by the fact that the increase in cell temperature reduces the band gap of the semiconductor, which lowers the open circuit voltage. On the other hand, the increase in temperature tends to increase the short-circuit current logarithmically. This is due to the improved mobility of charge carriers at high temperatures. The combination of these two effects results in a decrease in the maximum power produced by the PV/T system when the cell temperature increases. This can be seen in Fig. 4 by moving the maximum power point towards lower current and voltage values. The combination of these two effects results in a decrease in the maximum power produced by the PV/T system when the cell temperature increases. This led to an electrical power of 179.6 W at minimum cell temperature and 131 W at maximum temperature.

Table 4
Experimental validation of the coupled PV/T-electrolyzer model.

I ($T_{electro}$ = **80°C**)	V_{exp} Ref [33].	V_{num} (Present work)
0.1428	1.6857	1.6946
0.2857	1.7333	1.7445
0.4285	1.7620	1.7739
0.5714	1.7896	1.7923
0.8571	1.8275	1.8323
1.0000	1.8500	1.8502
1.2857	1.8733	1.8807
1.7142	1.9066	1.9155
2.0000	1.9333	1.9413
2.5714	1.9733	1.9839
3.0000	2.0071	2.0135
4.0000	2.0821	2.1047
Relative error (%)		**0.54**
RMSE (%)		**1.28**

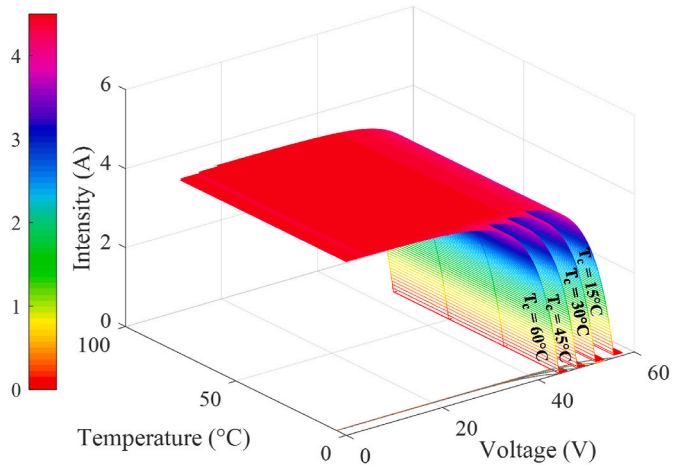

Fig. 3. Influence of temperature on the current-voltage characteristics of PV/T.

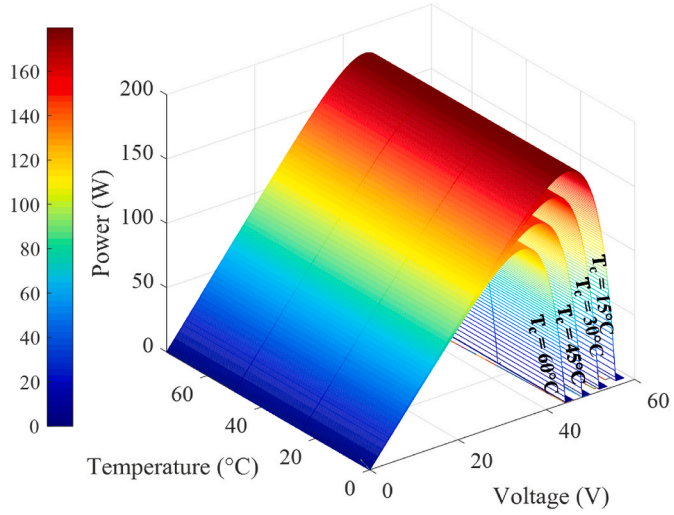

Fig. 4. Influence of temperature on PV/T output voltage and power.

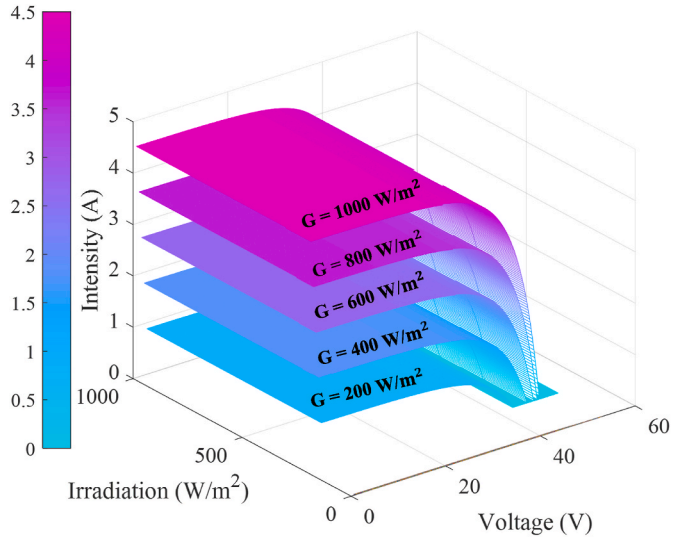

Fig. 5. Influence of solar irradiation on the current-voltage characteristic at the PV/T output.

- Influence of solar radiation on current-voltage and system power characteristics

Fig. 5 shows the influence of solar irradiation on the current-voltage characteristic of the PV/T hybrid solar system. The observation made is that when the solar irradiation increases, the output current of the PV/T system increases almost linearly. With a solar irradiation of 200 W/m^2, the maximum current is 0.88 and the maximum voltage is 43.34 V. Further at 1000 W/m^2, the maximum current is 4.501 and the maximum voltage is 50.72 V. This trend continues. explained by the fact that the increase in the flow of photons incident on the photovoltaic cells generates more electron-hole pairs, which results in an increase in the short-circuit current. The low variation in voltage is explained by the fact that the open circuit voltage of the PV cells depends logarithmically on the short-circuit current, which itself varies linearly with irradiation. Also visible in Fig. 6, it is seen that the output power of the PV/T system increases almost linearly with solar irradiation. A maximum electrical power of 152.4 W is reached for solar irradiation at 1000 W/m^2. This results from the combination of the linear increase in current and the small increase in voltage with irradiation.

- Evaluation of the thermal and electrical performances of the PV/T system

Fig. 7 shows the influence of cell temperature and solar irradiation on the electrical power output from the PV/T. At 20 °C and 200 W/m^2 cell temperature and solar irradiation respectively, the electrical power is 29.52 W. By maintaining this cell temperature at 20 °C, with solar irradiation at 1000 W/m^2, the electrical power is at 147.6 W. On the other hand, by setting the solar irradiation at 1000 W/m^2, with a cell temperature at 50 °C, the electrical power drops by almost 21 W. Then decreasing by 4.32 W in the case of irradiation fixed at 200 W/m^2 and a cell temperature leaving from 20 °C to 25.2 °C. This visualization reveals that as the temperature of the PV cells increases, the electrical power of the PV/T system decreases significantly and increases more significantly with solar radiation. It can be established that the negative effect of temperature on electrical power is all the more marked as solar irradiation is high. Hence the need for a cooling fluid (water in our case) used to reduce the temperature of the cells. The influence of the outlet fluid temperature and solar irradiation on the thermal power is visualized in Fig. 8. It shows the relationship between the overall irradiation, the water outlet temperature and the thermal power of the system. Increased thermal power can be observed when solar irradiation increases. A minimum thermal power of 129.8 W is reached at 200 W/ m^2

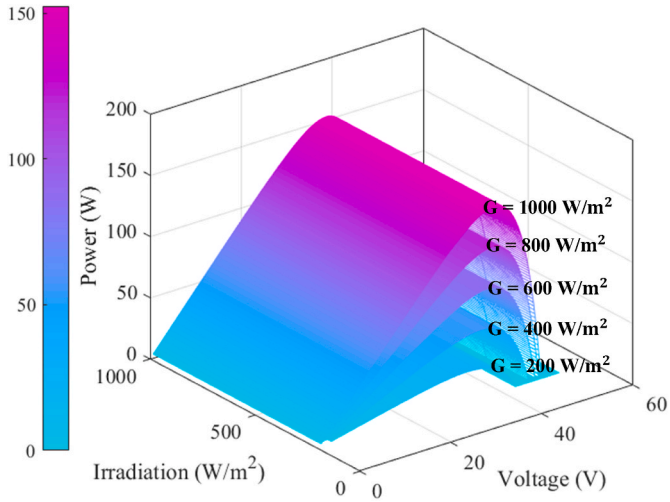

Fig. 6. Influence of solar irradiation on PV/T output voltage and power.

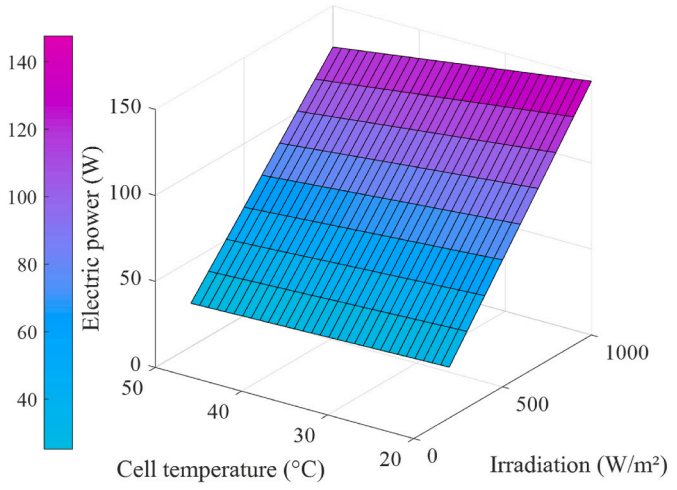

Fig. 7. Influence of cell temperature and irradiation on the electrical power of PV/T.

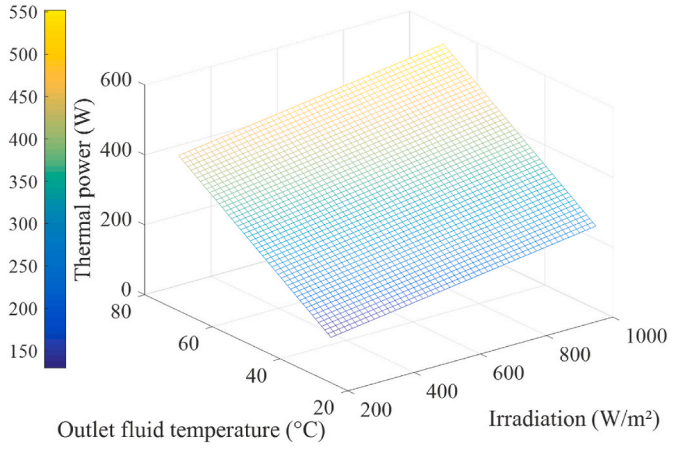

Fig. 8. Influence of the outlet fluid temperature and solar irradiation on the thermal power of the PV/T.

with an outlet water temperature of 25 °C. And a maximum thermal power of 551.9 W is reached at 1000 W/ m^2 with a fluid outlet temperature of 70 °C. This is explained by the fact that the higher the irradiation, the heating of the cells is significant, and the temperature at the water outlet is high. And the greater the temperature difference between the inlet and outlet of the water, the greater the heat transfer. This results in an increase in thermal power. The cell cooling system with water directly promotes an increase in the output voltage as well as the electrical output power of the PV/T. It could also be explained by the fact that reducing the temperature of the PV cells reduces the thermal agitation of the electrons, which facilitates their separation in the transition zone (PN junction) and therefore increases the voltage.

- Evaluation of the current-voltage characteristics of the PV/T-electrolyzer system

The study of the current-voltage characteristics of the system is crucial to understand and optimize the operation of a PV/T-electrolyzer system. These characteristics make it possible to evaluate the efficiency of the conversion of solar energy into electrical energy and hydrogen produced by electrolysis. Fig. 9 (a) and **9. (b)** present the current-voltage characteristics of the PV/T/Electrolyzer couple and the electrolyzer respectively. That of the electrolyzer has a non-linear appearance, with a progressive increase in voltage as the current increases. It presents a maximum power point which will correspond to the optimal operation of the PV/T-electrolyzer coupling. Has a maximum current of 4.43 A and 1.71 V maximum voltage. These values are influenced by overvoltages linked to oxidation and reduction reactions, as well as by the internal resistance of the electrolyzer. This operating point of the PV-electrolyzer system corresponds to the intersection between the IV characteristics of the PV/T photovoltaic generator and those of the electrolyzer. This point represents the current and voltage values for which the system operates optimally.

In Fig. 10, the evaluation of the produced hydrogen flow rate as a function of (a) current density and (b) local time is presented. The relationship between the current density applied to the electrolyzer and the volumetric flow rate of hydrogen produced is linear. At a current density of 100 mA/cm^2, the flow rate of hydrogen produced is 0.016 m^3/h, and at 174 mA/cm^2 the flow rate is 0.028 m^3/h which represents the flow rate obtained at the hour (12h) of maximum sunshine as shown in Fig. 10b. Thus, at hours (6 a.m.–9 a.m. and 3 p.m.–6 p.m.) when solar irradiation is low, the hydrogen flow rate reaches values below 0.015 m^3/h. There is therefore a strong dependence on the electricity production of PV/T. This corroborates the observations made in studies [17, 18], which showed that hydrogen production directly depends on the electricity production of the PV/PV-T system. In addition, these values are of the same order of magnitude as those reported in the study [17] of the literature, where flow rates of 0.55 Nm^3/h and 0.675 Nm^3/h were obtained respectively with PV and wind-electrolyzer systems. the results obtained clearly demonstrate the linear relationship between the

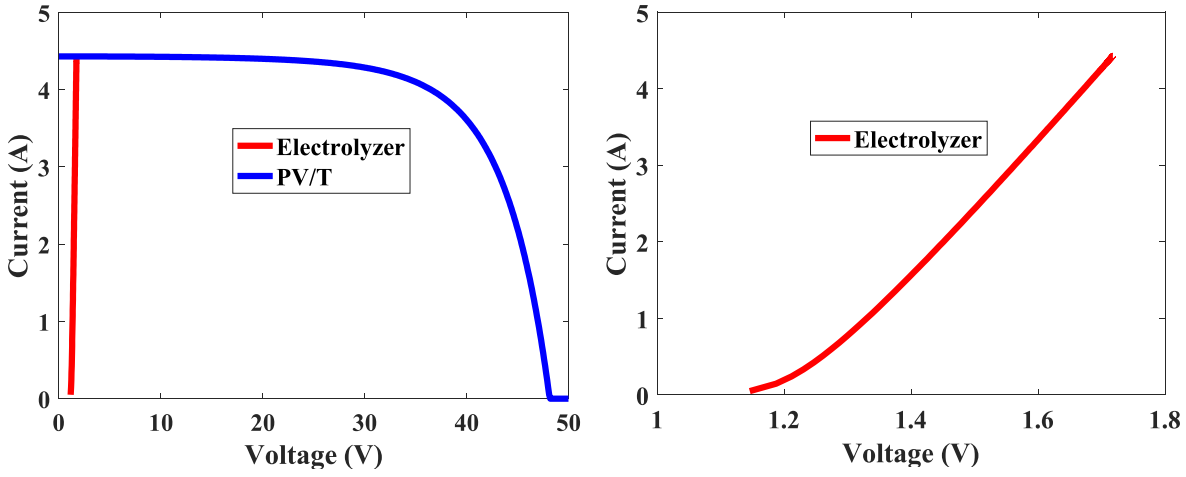

Fig. 9. Current-voltage characteristics (a) of the PV/T/Electrolyzer couple (b) of the electrolyzer.

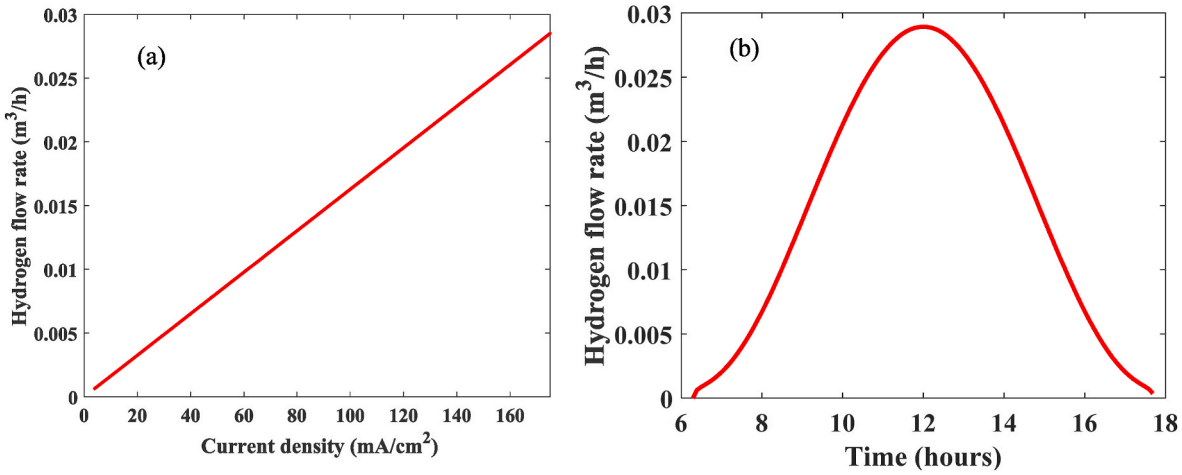

Fig. 10. Evaluation of the hydrogen flow rate produced as a function of (a) current density and (b) local time.

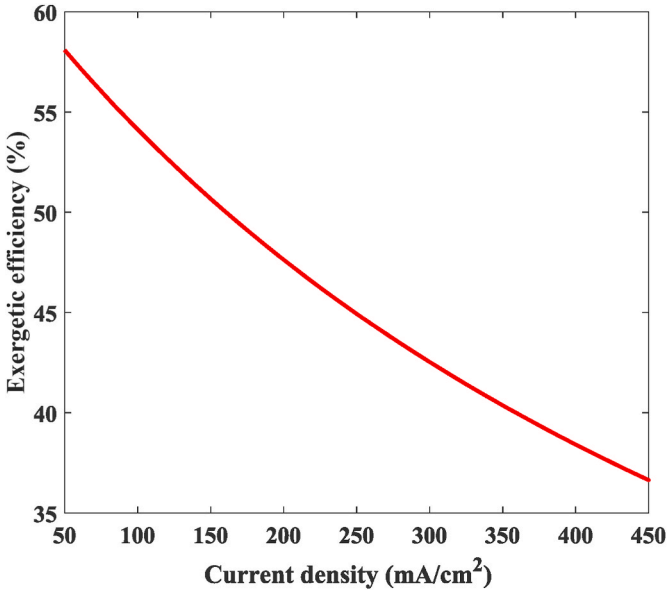

Fig. 11. Variation of exergy efficiency as a function of current density.

electric current and the hydrogen flow, as well as the variation in the electrical production of the PV/T depending on the sunshine during the day, which directly conditions the flow of hydrogen. hydrogen produced by the electrolyzer. This observation is consistent with the results of studies [19–21] in the literature, which also pointed out that the output voltage of electrolysis is strongly affected by electrolyzer parameters such as current density.

- Exergy sensitivity analysis of some system parameters

Exergy sensitivity analysis makes it possible to optimize the design of the PV/T-electrolyzer system. Optimization of these design parameters would improve the overall exergy efficiency of the system. Thus, the exergy efficiency makes it possible to evaluate to what extent the electrolysis system uses electrical energy to produce hydrogen and oxygen. Fig. 11 shows the variation of exergy efficiency as a function of current density. The solar radiation incident on the PV/T is set at 1000 W/m^2 and the temperature of the electrolyser is set at 60 °C and a flow rate of 3.5×10^{-3}m^3/h. The observation is that the exergy efficiency of electrolysis decreases as the current density increases. Thus, at low current density, polarization losses are reduced, but the hydrogen production rate is low, which limits performance. exergy. However, at high current density, polarization losses increase, reducing the exergy efficiency. Hence, an optimal current density (200 mA/cm^2 for 47 % exergy efficiency) lying in an intermediate range, neither too low nor too high is recommended. This may involve working at an intermediate current density, where flow rate is acceptable and exergy efficiency remains relatively high. In Fig. 12, the effect of exergy efficiency as a function of electrolyzer temperature is presented. According to this figure, the exergy efficiency of the electrolyzer increases significantly with temperature. This trend is explained by the fact that at higher temperatures, the kinetics of electrochemical reactions at the electrode accelerate, which reduces overvoltages and improves the efficiency of the process. The ionic conductivity of the electrolyte also increases with temperature, reducing ohmic losses. This results in an improvement in the reversible potential and therefore in the exergy efficiency. A higher operating temperature (around 50–60 °C for greater efficiency) exergy of 39 %) is generally desirable to improve exergy efficiency. But, although increasing temperature improves exergy efficiency, it can have impacts on other aspects of the system, such as the energy consumption of the heating system. Also, temperatures that are too high can cause problems with degradation of the electrolyzer materials. A compromise must therefore be found between exergy efficiency and other performance criteria of the electrolysis system. Fig. 13 presents the variation of

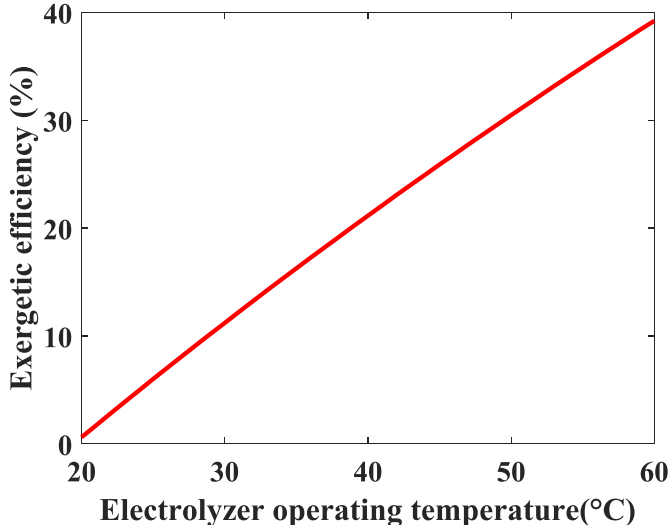

Fig. 12. Variation of exergy efficiency as a function of electrolyzer temperature.

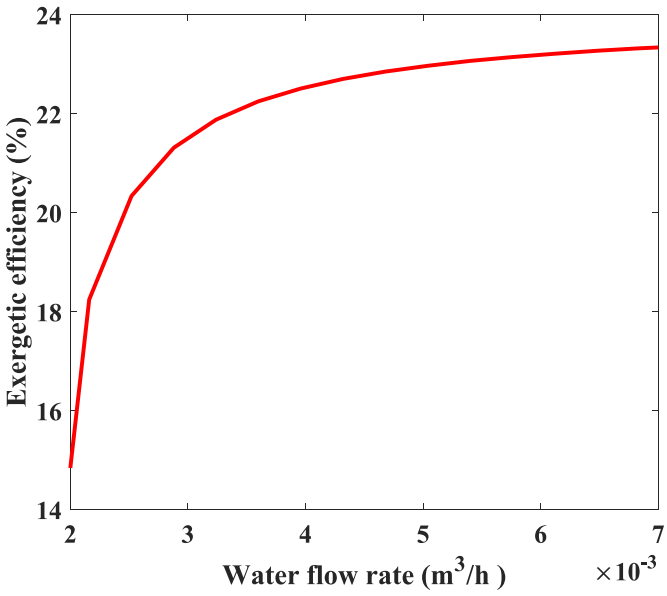

Fig. 13. Variation of exergy efficiency as a function of water flow in the electrolyzer.

the exergy efficiency as a function of the water flow in the electrolyzer. The exergy efficiency of the electrolyzer increases significantly as the water flow increases to an efficiency threshold where it tends to stabilize. This is explained by the fact that at a low water flow, the transport of reagents (water, ions) towards the electrodes is limited, which leads to concentration overvoltages and the evacuation of gas bubbles (hydrogen and oxygen) produced at the electrodes is less effective. Beyond this threshold ($5.7 \times 10^{-3} m^3/h$), increasing the water flow no longer brings significant improvement in performance. This is probably explained by the appearance of other limiting phenomena, such as the increased energy consumption of the circulation pump. Table 5 presents the results of the optimal parameters obtained. The literature [16, 19–21] confirms this multi-criteria optimization approach to find the optimal sizing and particularly the authors [16] with a PV-electrolyzer system. But these results provide more information that exergy analysis and multi-objective optimization can identify exergy losses in the system and optimize system parameters.

- Monthly assessment of hydrogen and oxygen production

Fig. 14.a and Fig. 14b presents the monthly evaluation of the production of hydrogen and oxygen delivered by the hybrid solar PV/T-electrolyzer system. The monthly production of hydrogen and oxygen reaches the maximum values 4.85 m^3 and 2.42 m^3 respectively in February. And the minimum values of 1.87 m^3 and 0.93 m^3 respectively for hydrogen and oxygen in the month of July. This strong seasonal variation is probably explained by fluctuations in the electricity production of the PV/T system which supplies the electrolyzer. These results show the importance of taking into account seasonal variations in renewable electricity production to correctly size a hydrogen production system by electrolysis. The maximum hydrogen productions that you report (4.85 m^3/month) are of the same order of magnitude as those observed in the study [24], which obtained monthly productions of up to 6 m^3. This highlights the crucial importance of taking into account these seasonal fluctuations when designing and sizing such renewable production systems.

Table 5
Optimal system parameters.

Exergy efficiency (%)	39	47	23.1
Settings	*Electrolyzer temperature*	*Current density*	*Water flow in the electrolyzer*
Parameter values	**60°C**	**200mA/cm²**	**5.7×10^{-3} m^3/h**

- Challenges and limitations of technology

Although PV/T-electrolyzer technology has many advantages in terms of production performance and carbon emissions, CO_2 reduced, it faces several major challenges that must be overcome to enable successful deployment on a large scale.

First, the long-term reliability and durability of the system must be improved. Components, particularly the electrolyzer, may experience premature degradation with intermittent operation or frequent charge/discharge cycles. This could significantly reduce the lifespan of the system and limit its economic viability. Advances in materials and manufacturing techniques are necessary to increase the robustness and longevity of these technologies.

Second, challenges related to integration into the electricity grid must be overcome. The intermittency of solar production can cause disruptions on the grid and require the development of storage and intelligent energy management solutions. In addition, increasing the share of green hydrogen in the overall energy mix implies the establishment of suitable distribution and refueling infrastructures, which represents a considerable investment.

Finally, further progress is needed in component design and system modeling to further optimize their performance and efficiency. In particular, further studies are required to assess the impact of environmental conditions, design parameters and control strategies on overall hydrogen and heat production.

Despite these challenges, the potential of hybrid PV/T-electrolyzer systems for large-scale green hydrogen production remains significant. Continued efforts in research, technology development and business model innovation will be essential to overcome these obstacles and enable wider adoption of this sustainable solution.

4. Conclusion

Water electrolysis is an efficient and clean way to produce hydrogen and oxygen from water and electricity. This is a key process for the development of a sustainable hydrogen economy. This digital study is therefore a contribution to the production of healthy and sustainable hydrogen with the source of a new hybrid photovoltaic and thermal solar system. There is therefore double production in addition to electricity, heat which can be used in hospitals for heating, electricity and oxygen supply. And in several sectors of activity. After experimental validation, the effect of operating parameters such as operational operating temperature of the electrolyzer, current density and mass flow rate of water in the electrolyzer on the exergy performance are analyzed. This article reveals that:

- The negative effect of temperature on electrical power is all the more marked as solar irradiation is high;
- That with a maximum operating point of the PV/T-electrolyzer system at 4.43 A and 1.718 V, hydrogen is obtained;
- The relationship between the current density applied to the electrolyzer and the volumetric flow rate of hydrogen produced is linear. But at high density, a slight deviation from linearity may appear due to overvoltage phenomena and losses, limiting the exergy yield;
- The renewal of the fluid allows better dissipation of the heat generated by the irreversible processes in the electrolyzer;
- Beyond this threshold ($5.7 \times 10^{-3} m^3/h$), increasing the water flow no longer brings significant improvement in performance;

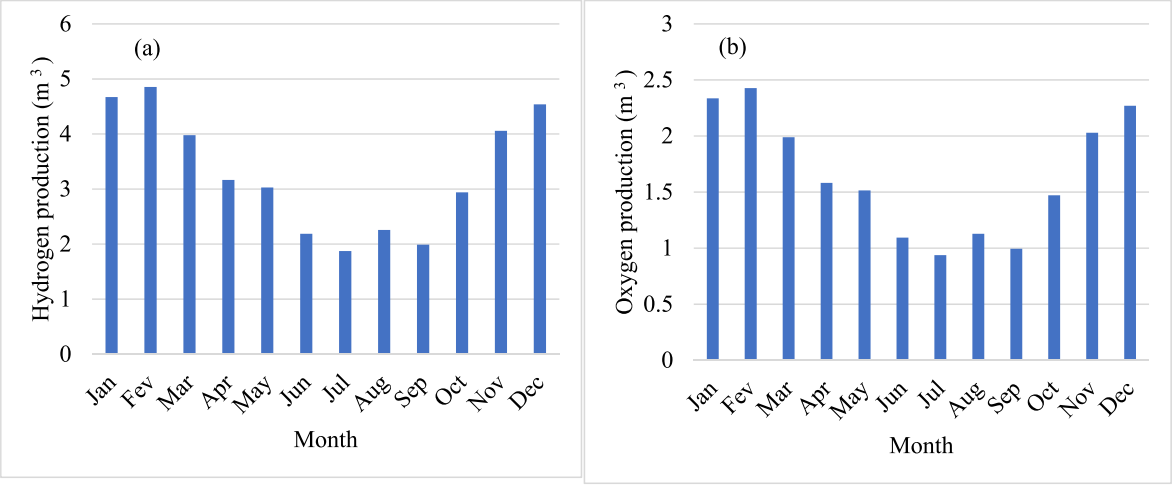

Fig. 14. Evaluation of monthly hydrogen and oxygen production.

- With a water flow of 5.7 $\times 10^{-3}$ m^3/h, a current density of 200 **mA/cm²** and an electrolyzer temperature of 60 °C, the monthly production of hydrogen and oxygen reaches the maximum values of 4.85 m^3 and 2.42 m^3 respectively.

The results of this study provide valuable information to guide the development of sustainable energy solutions, integrating the production of electricity, hydrogen, oxygen and heat from a hybrid photovoltaic and thermal solar system. In perspective, this study could be improved by including load and demand management in the analysis process and storage as well as economic analysis are strongly recommended. Additionally, limited long-term reliability and durability, grid integration challenges, and the need for continued design and modeling optimization efforts represent the main obstacles to large-scale deployment of this technology. However, its potential remains significant and requires continued investment in research and development to overcome these challenges.

Funding statement

This research did not receive any specific grant from funding agencies in the public, commercial, or not-for-profit sectors.

Nomenclature

G	Inclined solar radiation (W/m^2)
C_P	Water specific heat (J/kg.K)
k	Specific heat
n	Number of electrons
P	Partial pressure
z	Stoichiometric coefficient of electron
k	The constant Boltzmann
q	The elementary charge of the electron
Tc	The absolute temperature of the sun cell
I	current density
I_0	Saturation current
F	Faraday's constant
T	Temperature
$\dot{m}$	Mass flow rate (kg/s)
V	Voltage
Ex, ex	Exergy
$\dot{E}x$	Rate of exergy
FC	fuel cell
PEM	Polymer electrolyte membrane
PV	Photovoltaics
PV/T	Photovoltaic/Thermal
RMSE	Root Mean Squared Error
Subscripts	

(*continued on next column*)

(*continued*)

A	Ambient
in,i	Inlet
electric	Electric
F	Fluid
o	Outlet
rev	Reversible
th	Thermal
ohm	Ohmic
act	Activation
number	Digital
electro	Electrolyzer

CRediT authorship contribution statement

Armel Zambou Kenfack: Writing – review & editing, Writing – original draft, Validation, Software, Resources, Methodology, Investigation, Formal analysis, Conceptualization. **Modeste Kameni Nematchoua:** Writing – review & editing, Writing – original draft, Visualization, Validation, Supervision, Conceptualization. **Venant Sorel Chara-Dackou:** Writing – review & editing, Writing – original draft, Visualization, Validation, Supervision, Software, Conceptualization. **Elie Simo:** Writing – review & editing, Writing – original draft, Visualization, Validation, Supervision, Conceptualization.

Declaration of competing interest

The authors declare that they have no known competing financial interests or personal relationships that could have appeared to influence the work reported in this paper.

Data availability

I've shared the link to the data I used, citing in the references

References

[1] B.A.P. Pemi, D. Njomo, R. Tchinda, J.C. Seutche, A.Z. Kenfack, M.H. Babikir, V. S. Chara- Dackou, Sectoral assessment of the energy, water, waste and land nexus in the sustainability of agricultural products in Cameroon, Sustainability 16 (2) (2024) 565, https://doi.org/10.3390/su16020565.

[2] S.R. Arsad, A.Z. Arsad, P.J. Ker, M.A. Hannan, S.G. Tang, S.M. Goh, T.M.I. Mahlia, Recent advancement in water electrolysis for hydrogen production: a comprehensive bibliometric analysis and technology updates, Int. J. Hydrogen Energy 60 (2024) 780–801, https://doi.org/10.1016/j.ijhydene.2024.02.184.

[3] M. Awad, A. Said, M.H. Saad, A. Farouk, M.M. Mahmoud, M.S. Alshammari, A. I. Omar, A review of water electrolysis for green hydrogen generation considering PV/wind/hybrid/hydropower/geothermal/tidal and wave/biogas energy systems , economics analysis , and its application, Alex. Eng. J. 87 (2024) 213–239, https://doi.org/10.1016/j.aej.2023.12.032.

[4] E.A. Sarsah, A.K. Sunnu, A.R. Bawa, Assessment of the technical-economic feasibility of solar-hydrogen hybrid systems: a review of recent studies, iEnergy 3 (1) (2024) 28–38. https://doi:10.23919/IEN.2024.0004.
[5] Q. Hassan, V.S. Tabar, A.Z. Sameen, H.M. Salman, M. Jaszczur, A review of solar-based green hydrogen production; techniques and methods, Recovery and Energy Systems 11 (1) (2024) 20220134, https://doi.org/10.1515/ehs-2022-0134.
[6] Z. Li, S. Fang, H. Sun, R.J. Chung, X. Fang, J.H. He, Solar hydrogen, Adv. Energy Mater. 13 (8) (2023) 2203019, https://doi.org/10.1002/aenm.202203019.
[7] B. Laoun, A. Khellaf, M.W. Naceur, Kannan , AM Modeling of solar photovoltaic-polymer electrolyte membrane electrolyzer direct coupling for hydrogen generation, Int. J. Hydrogen Energy 41 (24) (2016) 10120–10135, https://doi.org/10.1016/j.ijhydene.2016.05.041.
[8] M.A. Abdelkareem, A.A. Abdelghafar, M. Mahmoud, E.T. Sayed, M.S. Mahmoud, A. H. Alami, Olabi , AG Optimized solar photovoltaic-powered green hydrogen : current status , recent advancements , and barriers, Sol. Energy (2023) 112072, https://doi.org/10.1016/j.solener.2023.112072.
[9] B.A.M. Nouadje, P.T. Kapen, V. Chegnimonhan, R. Tchinda, Techno-economic analysis of a grid/fuel cell/PV/electrolyzer system for hydrogen and electricity production in the countries of African and Malagasy council for higher education (CAMES), Energy Strategy Rev. 53 (2024) 101392, https://doi.org/10.1016/j.esr.2024.101392.
[10] V.S. Chara- Dackou, D. Njomo, R. Tchinda, Y.S. Kondji, H.M. Babikir, N. H. Chopkap, B.A.P. Pemi, A.Z. Kenfack, Mbouombouo NI Sensitivity analysis of the thermal performance of a parabolic trough concentrator using Al2O3 and SiO2/ Vegetable oil as heat transfer fluid, Heliyon (2024) e23978, https://doi.org/10.1016/j.heliyon.2024.e23978. ISSN 2405-8440.
[11] K. Liu, N. Wang, Y. Pan, T.A. Alahmadi, S.A. Alharbi, G.K. Jhanani, K. Brindhadevi, Photovoltaic thermal system with phase changing materials and MWCNT nanofluids for high thermal efficiency and hydrogen production, Fuel 355 (2024) 129457, https://doi.org/10.1016/j.fuel.2023.129457.
[12] M. Sangeetha, B. Gavurová, M. Sekar, M.M. Al-Ansari, L.A. Al- Humaid, Q.H. Le, G. K. Jhanani, Production of hydrogen as value added product from the photovoltaic thermal system operated with graphene nanoparticles : an experiment study, Fuel 334 (2023) 126792, https://doi.org/10.1016/j.fuel.2022.126792.
[13] A.Z. Kenfack, K.M. Nematchoua, E. Simo, Konchou Fat, M.H. Babikir, B.A.P. Pemi, Chara- Dackou VS Techno-economic and environmental analysis of a hybrid PV/T solar system based on vegetables and synthetics oils coupled with TiO2 in Cameroon, Heliyon (2024) e24000, https://doi.org/10.1016/j.heliyon.2024.e24000.
[14] M. Benghanem, A. Mellit, H. Almohamadi, S. Haddad, N. Chettibi, A.M. Alanazi, A. Alzahrani, Hydrogen production methods based on solar and wind energy : has review, Energies 16 (2) (2023) 757, https://doi.org/10.3390/en16020757.
[15] M.M. Maseer, F.B. Ismail, H.A. Kazem, L.C. Wai, Al- Gburi, KAH Optimal evaluation of photovoltaic -thermal solar collectors cooling using a half -tube of different diameters and lengths, Sol. Energy 267 (2024) 112193, https://doi.org/10.1016/j.solener.2023.112193.
[16] C. Mokhtara, B. Negrou, N. Settou, A. Bouferrouk, Y. Yao, Design optimization of grid-connected PV- Hydrogen for energy prosumers considering sector coupling paradigm : case study of a university building in Algeria, Int. J. Hydrogen Energy 46 (75) (2021) 37564–37582, https://doi.org/10.1016/j.ijhydene.2020.10.069.
[17] E. Nkanga, D. Ndoh, J. Ntonda, A. Nanfak, M. Mekouebe, F. Lontsi, Modeling of hydrogen production in an alkaline electrolyser system connected with a solar photovoltaic panel or a wind turbine: case study ; douala- Cameroon, J. Power Energy Eng. 9 (2021) 1–18, https://doi.org/10.4236/jpee.2021.910001.
[18] M. Nasser, H. Hassan, Assessment of standalone streetlighting energy storage systems based on hydrogen of hybrid PV/electrolyzer/fuel cell/desalination and PV/batteries, J. Energy Storage 63 (2023) 106985, https://doi.org/10.1016/j.est.2023.106985.
[19] Y.F. Liu, Q. Su, H. Zhang, Cai, CP Optimization of photovoltaic-electrolyzer system by direct coupling, Appl. Mech. Mater. 44 (2011) 1578–1582. https://doi.org/10.4028/www.scientific.net/AMM.44-47.1578.
[20] N. Wang, Y. Guo, L. Liu, S. Shao, Numerical assessment and optimization of photovoltaic-based hydrogen-oxygen Co-production energy system: a machine learning and multi-objective strategy, Renew. Energy 227 (2024) 120483, https://doi.org/10.1016/j.renene.2024.120483.
[21] M. Nasser, M.M. Awad, A.A. Hassan, 4E assessment of all -day clean electricity generation systems based on green hydrogen integrated system using PV and PVT solar collectors and wind turbines, Int. J. Hydrogen Energy (2024), https://doi.org/10.1016/j.ijhydene.2024.05.089.
[22] S. Sadeghi, M. Ameri, Exergy analysis of photovoltaic panels -coupled solid oxide fuel cell and gas turbine -electrolyzer hybrid system, J. Energy Resour. Technol. 136 (3) (2014) 031201, https://doi.org/10.1115/1.4026313.
[23] M. Gül, E. Akyüz, Hydrogen generation from a small-scale solar photovoltaic thermal (PV/T) electrolyzer system: numerical model and experimental verification, Energies 13 (11) (2020) 2997, https://doi.org/10.3390/en13112997.
[24] A. Khalilnejad, A. Sundararajan, A. Abbaspour, A. Sarwat, Optimal operation of combined photovoltaic electrolyzer systems, Energies 9 (5) (2016) 332, https://doi.org/10.3390/en9050332.
[25] S. Touili, A. Bouaichi, A.A. Merrouni, A.I. Amrani, A. El Amrani, Y. El Hassouani, C. Messaoudi, Performance analysis and economics competitiveness of 3 different PV technologies for hydrogen production under the impact of arid climatic conditions of Morocco, Int. J. Hydrogen Energy 47 (74) (2022) 31596–31613, https://doi.org/10.1016/j.ijhydene.2022.07.088.
[26] Arif Karabuga, et al., " Exergy , economic and environmental analyzes of the renewable energy assisted hydrogen , cooling and electricity production: a case study.", Int. J. Hydrogen Energy (2024), https://doi.org/10.1016/j.ijhydene.2024.01.195.
[27] A. Fouda, A. Khaliq, H.F. Elattar, A. Al- Zahrani, B.A. Almohammadi, H.A. Refaey, Evaluation of a concentrated solar power- driven system designed for combined production of cooling and hydrogen, Case Stud. Therm. Eng. 59 (2024) 104567, https://doi.org/10.1016/j.csite.2024.104567.
[28] A. Khaliq, H.A. Refaey, M.A. Alharthi, B.A. Almohammadi, System development for production and onsite use of hydrogen in wet-ethanol fueled HCCI engine for cogeneration of power and cooling, Case Stud. Therm. Eng. 55 (2024) 104153, https://doi.org/10.1016/j.csite.2024.104153.
[29] M. El- Shafie, Hydrogen production by water electrolysis technologies: a review, Results in Engineering 101426 (2023), https://doi.org/10.1016/j.rineng.2023.101426.
[30] A. Khaliq, A. Al- Zahrani, B.A. Almohammadi, A.M. Alsharif, H.A. Refaey, Proposal and analysis of a concentrating photovoltaic-driven system for combined production of electricity , hydrogen , and low-temperature refrigeration, Case Stud. Therm. Eng. 51 (2023) 103565, https://doi.org/10.1016/j.csite.2023.103565.
[31] E. Özgirgin, Y. Devrim, A. Albostan, Modeling and simulation of a hybrid photovoltaic (PV) module- electrolyzer -PEM fuel cell system for micro-cogeneration applications, Int. J. Hydrogen Energy 40 (44) (2015) 15336–15342, https://doi.org/10.1016/j.ijhydene.2016.08.224.
[32] R.K. De, A. Ganguly, Modeling and analysis of a solar thermal- photovoltaic -hydrogen-based hybrid power system for running a standalone cold storage, J. Clean. Prod. 293 (2021) 126202, https://doi.org/10.1016/j.jclepro.2021.126202.
[33] T.M. Ismail, K. Ramzy, B.E. Elnaghi, M.N. Abelwhab, M. Abd El-Salam, Using MATLAB to model and simulate a photovoltaic system to produce hydrogen, Energy Convers. Manag. 185 (2019) 101–129, https://doi.org/10.1016/j.enconman.2019.01.108.
[34] K.A. Zambou, M.K. Nematchoua, E. Simo, M.N. Mfoundikou, J.V.K. Fosso, M. H. Babikir, Chara- Dackou , VS Exergetic optimization of some design parameters of the hybrid photovoltaic/thermal collector with bi- fluid air/ternary nanofluid ($CuO/MgO/TiO_2$), SN Appl. Sci. 5 (8) (2023) 226, https://doi.org/10.1007/s42452-023-05455-z.
[35] A.T. Zamorano, F.A. Cataño, A. Arunachalam, D. Oyarzún, R. Henriquez, P. Valdivia, H. Gómez, Green hydrogen production by photovoltaic-assisted alkaline water electrolysis : a review on the conceptualization and advancements, Int. J. Hydrogen Energy (2024), https://doi.org/10.1016/j.ijhydene.2024.04.333.
[36] X. Ding, Y. Zhou, N. Zheng, Y. Wang, M. Yang, L. Duan, Energy, exergy , and economic analyzes of a novel liquid air energy storage system with cooling , heating , power, hot water, and hydrogen cogeneration, Energy Convers. Manag. 305 (2024) 118262, https://doi.org/10.1016/j.enconman.2024.118262, 2024.
[37] X. Qi, O. Kochan, Z. Ma, P. Siarry, G. Królczyk, Z. Li, Energy, exergy , exergoeconomic and exergoenvironmental analyzes of a hybrid renewable energy system with hydrogen fuel cells, Int. J. Hydrogen Energy 52 (2024) 617–634, https://doi.org/10.1016/j.ijhydene.2023.07.163.
[38] F.E. Sapnken, F. Posso, M.T. Kibong, J.G. Tamba, The potential of green hydrogen fuel as an alternative in Cameroon's road transport sector, Int. J. Hydrogen Energy 49 (2024) 433–449, https://doi.org/10.1016/j.ijhydene.2023.08.339.
[39] D. H idouri, R. Marouani, A. Cherif, Modeling and simulation of a renewable energy PV/PEM with green hydrogen storage, Eng. Technol. Appl. Sci. Res. 14 (1) (2024) 12543–12548, https://doi.org/10.48084/etasr.6492.
[40] C.H. Li, X.J. Zhu, G.Y. Cao, S. Sui, M.R. Hu, Dynamic modeling and sizing optimization of stand-alone photovoltaic power systems using hybrid energy storage technology, Renew. Energy 34 (3) (2009) 815–826, https://doi.org/10.1016/j.renene.2008.04.018.
[41] M. Mehrpooya, S. Daviran, Dynamic modeling of a hybrid photovoltaic system with hydrogen/air PEM fuel cell, Iran. J. Energy Environ. 4 (2) (2013), https://doi.org/10.5829/idosi.ijee.2013.04.02.05.
[[42] A.Z. Kenfack, M.K. Nematchoua, E. Simo, V.S. Chara- Dackou, B.A.P. Pemi, Performance improvement of hybrid photovoltaic/thermal systems : a metaheuristic artificial intelligence approach to select the best model using 10E analysis, Solar Energy Advances 100061 (2024), https://doi.org/10.1016/j.seja.2024.100061.
[43] M. Aravindan, P. Kumar, Hydrogen towards sustainable transition: a review of production, economic , environmental impact and scaling factors, Results in Engineering 101456 (2023), https://doi.org/10.1016/j.rineng.2023.101456.